PROCEEDINGS OF SCIENCE

TTP24-034, P3H-24-066

QCD and electroweak corrections for single and double Higgs boson production at the LHC

Hantian Zhang[a,*]

[a] *Institut für Theoretische Teilchenphysik, Karlsruhe Institute of Technology (KIT), Wolfgang-Gaede Strasse 1, 76128 Karlsruhe, Germany*

E-mail: hantian.zhang@kit.edu

In these proceedings, we report recent progress of theoretical predictions for loop-induced Higgs boson production at the Large Hadron Collider (LHC). Our contributions include the next-to-leading order (NLO) QCD and electroweak corrections for single Higgs boson plus jet production, the NLO QCD corrections for single Higgs boson plus two jets production, and the NLO electroweak corrections for double Higgs boson production.

42nd International Conference on High Energy Physics (ICHEP2024)
18-24 July 2024
Prague, Czech Republic

*Speaker

PoS(ICHEP2024)074

1. Introduction

The precise determination of Higgs boson properties is one of the primary goals in particle physics, particularly in the LHC programme at CERN. For this purpose, single Higgs boson plus jets production and double Higgs boson production are key processes at the LHC, which can probe the Higgs boson transverse momenta (p_T^H) spectrum and the trilinear Higgs boson selfcoupling. They are sensitive to new physics effects beyond the Standard Model (SM), which are well-studied in the literature such as in Refs. [1–4]. To distinguish potential new physics effects, it is necessary to compute the higher-order QCD and electroweak (EW) radiative corrections for single Higgs boson plus jets and double Higgs boson production.

For single Higgs boson plus jet production (H + jet), the full NLO QCD corrections are computed in Refs. [5–7]. In particular, we have performed a dedicated study on top-quark mass (m_t) effects in Ref. [6]. Recent studies on top-quark mass effects on Higgs boson p_T^H spectrum can also be found in the literature such as in Refs. [8, 9]. The EW corrections via massless quark loops have been computed in Ref. [10], the corrections induced by a trilinear Higgs coupling in the large-m_t expansion have been calculated in Refs. [11]. We have computed the first full EW corrections involving top quarks in the large-m_t expansion in Ref. [12]. Recently, the beyond-the-SM effects on Higgs boson p_T^H spectrum have been explored in Refs. [13–15].

For single Higgs boson plus two jets production (H + 2 jets), we have computed the first NLO QCD corrections accounting for the top-quark mass effects in Ref. [6].

For double Higgs boson production (HH), the Yukawa-top and Higgs self-coupling corrections are addressed in Refs. [16–20], the EW corrections involving top quarks are computed analytically in the large-m_t expansion in Ref. [12], the factorisable EW corrections are computed analytically in Ref. [21], and the full EW corrections are computed numerically in Ref. [22].

In these proceedings, we summarise our contributions for these processes in Refs. [6, 12, 17, 21].

2. NLO QCD corrections for H + jet and H + 2 jets production

The computation of NLO QCD corrections for single Higgs boson plus jets production is performed in the `NNLOJET` framework, which is a parton-level event generators equipped with the antenna subtraction method [23]. The loop-induced matrix elements for H + jet and H + 2 jets contributing at the Born level and real corrections are provided by `OpenLoops2` [24], and the matrix elements for virtual corrections of H + jet are provided by `SecDec` [25]. The input parameters are $m_H = 125$ GeV, $m_t = 173.055$ GeV, $v = 246.219$ GeV, $\sqrt{s} = 13$ TeV, where v is the vacuum expectation value and $\sqrt{s}$ is center of mass energy at the LHC. We assume massless light quarks in initial and final states. The top-quark mass is renormalised in the on-shell scheme. Renormalisation and factorisation scales are chosen as $\mu_{\rm R,F} = \xi_{\rm R,F} \cdot H_T/2$ with $H_T = \sqrt{m_H^2 + p_{\rm T,H}^2} + \sum_j |p_{\rm T,j}|$, where the sum includes all final-state partons. Our central scale corresponds to $\xi_{\rm R,F} = (1, 1)$ and we determine scale uncertainties via 7-point factor-2 variations. We employ the $p_{\rm T,j} > 30\,$GeV cut for H + jet production, and $p_{\rm T,j_1} > 40\,$GeV and $p_{\rm T,j_2} > 30\,$GeV cuts for H + 2 jets production.

We study top-quark effects for these processes through three approaches: the heavy top limit (HTL), the so-called full theory approximation ($\rm FT_{approx}$) through a reweighting procedure based on the Born-level top-mass effects [26], and the exact top-mass dependence in the full SM QCD (only for H + jet production). We show the transverse momentum distribution for the Higgs

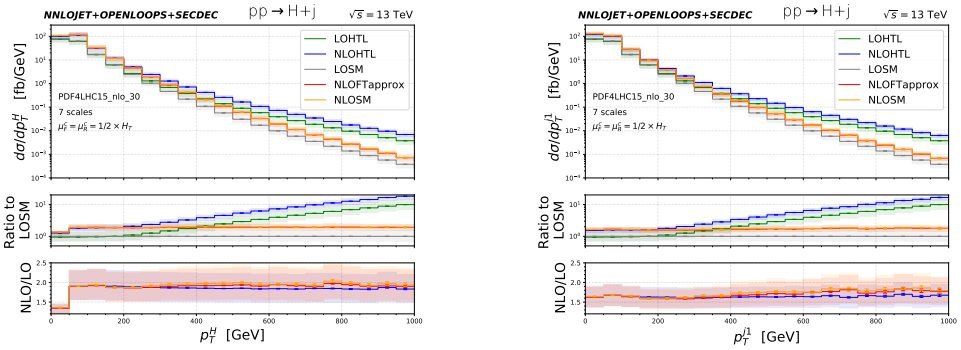

Figure 1: Transverse momentum distribution of the Higgs (left) and the hardest jet (right) in H + jet production. We show LO predictions in the full SM QCD (magenta) and the HTL (green) as well as NLO predictions in the HTL (blue), the $\mathrm{FT}_{\mathrm{approx}}$ (red) and the full SM QCD (orange). Shaded bands correspond to scale variations. Error bars indicate integration uncertainties. (from Ref. [6])

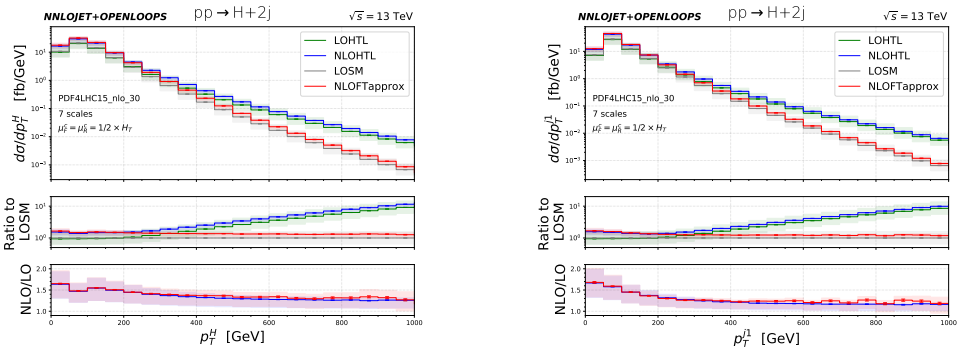

Figure 2: Transverse momentum distribution of the Higgs (left) and the hardest jet (right) in H + 2 jets production. Colour coding and labelling as in Fig. 1. (from Ref. [6])

σ[pb]		Inclusive $p_{T,H}$			$p_{T,H} > 300$ GeV		
		LO	NLO	K	LO	NLO	K
H + jet	HTL	$8.22^{+3.17}_{-2.15}$	$13.57^{+2.11}_{-2.09}$	1.65	$0.086^{+0.038}_{-0.024}$	$0.160^{+0.033}_{-0.030}$	1.86
	$\mathrm{FT}_{\mathrm{approx}}$	$8.56^{+3.30}_{-2.24}$	$14.06(1)^{+2.17}_{-2.16}$	1.64	$0.046^{+0.020}_{-0.013}$	$0.088^{+0.019}_{-0.017}$	1.91
	SM QCD	$8.56^{+3.30}_{-2.24}$	$14.15(7)^{+2.29}_{-2.21}$	1.65	$0.046^{+0.020}_{-0.013}$	$0.089(3)^{+0.020}_{-0.017}$	1.93
H + 2 jets	HTL	$2.87^{+1.67}_{-0.99}$	$4.33^{+0.59}_{-0.80}$	1.51	$0.120^{+0.071}_{-0.042}$	$0.160^{+0.012}_{-0.025}$	1.33
	$\mathrm{FT}_{\mathrm{approx}}$	$2.92^{+1.70}_{-1.01}$	$4.45(1)^{+0.63}_{-0.83}$	1.52	$0.068^{+0.040}_{-0.024}$	$0.092^{+0.008}_{-0.015}$	1.35
	SM QCD	$2.92^{+1.70}_{-1.01}$	–	–	$0.068^{+0.040}_{-0.024}$	–	–

Table 1: Integrated cross sections at LO and NLO QCD in the HTL and $\mathrm{FT}_{\mathrm{approx}}$ approximations and with full top-quark mass dependence (SM QCD) for H + jet and H + 2 jets production together with corresponding K-factors. Uncertainties correspond to the envelope of 7-point scale variations. On the left no further phase-space restrictions are considered, while on the right we require $p_{T,H} > 300$ GeV. (from Ref. [6])

boson (p_T^H) and the hardest jet (p_T^{j1}) for H + jet production in Fig. 1 and for H + 2 jets production in Fig. 2. The fiducial total cross section for H + jet and H + 2 jets production are presented in Table 1, including the results for boosted Higgs boson with $p_T^H > 300$ GeV. A detailed study of fiducial total cross sections with different p_T^H cuts ranging from 50 GeV to 800 GeV can be found in Ref. [6].

3. NLO EW corrections for H + jet and HH production

We perform analytic two-loop calculations for NLO EW corrections for H + jet and HH production by expansions in both low-energy and high-energy regions. In particular, as shown in Fig. 1, the major contribution for H + jet is from the low-energy region, which can be captured by a large-m_t expansion. A dedicated review on analytic expansion for EW corrections can be found in Ref. [27]. The factorisable contributions for $gg \to HH$ are analytically computed in Ref. [21].

Large-m_t expansion: We perform analytic calculations for the full top-quark-induced EW corrections for gluon-fusion H + jet ($gg \to gH$) and HH ($gg \to HH$) production through the large-m_t expansion. We assume the expansion hierarchy $m_t^2 \gg \xi_W m_W^2, \xi_Z m_Z^2 \gg s, t, m_W^2, m_Z^2, m_H^2$, where ξ_Z, ξ_W are the gauge-fixing parameters. The large-m_t expansion for bare two-loop amplitudes is performed to the order $1/m_t^8$. We perform parameter renormalisation for $\{e, m_W, m_Z, m_t, m_H\}$

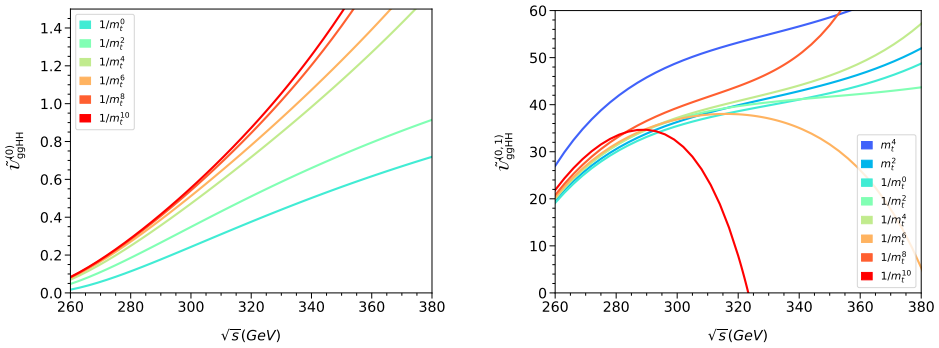

Figure 3: LO $\tilde{\mathcal{U}}^{(0)}_{\text{ggHH}}$ (left) and NLO EW $\tilde{\mathcal{U}}^{(0,1)}_{\text{ggHH}}$ (right) matrix elements plotted as a function of $\sqrt{s}$ for $gg \to HH$. Results are shown up to order $1/m_t^{10}$ (from Ref. [12]).

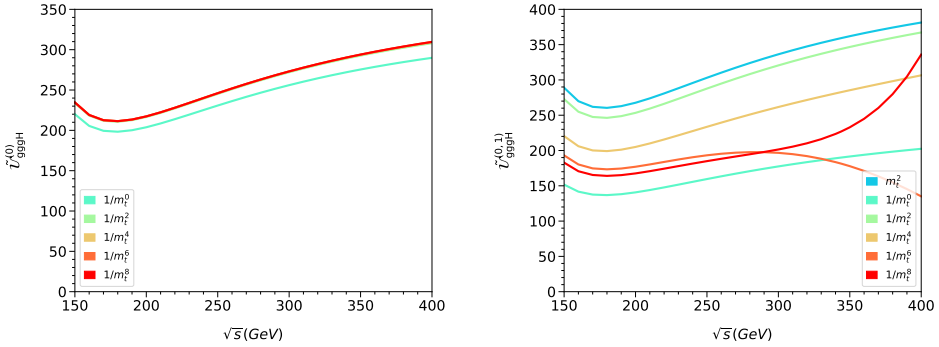

Figure 4: LO $\tilde{\mathcal{U}}^{(0)}_{\text{gggH}}$ (left) and NLO EW $\tilde{\mathcal{U}}^{(0,1)}_{\text{gggH}}$ (right) matrix elements plotted as a function of $\sqrt{s}$ for $gg \to gH$. Results are shown up to order $1/m_t^8$. (from Ref. [12])

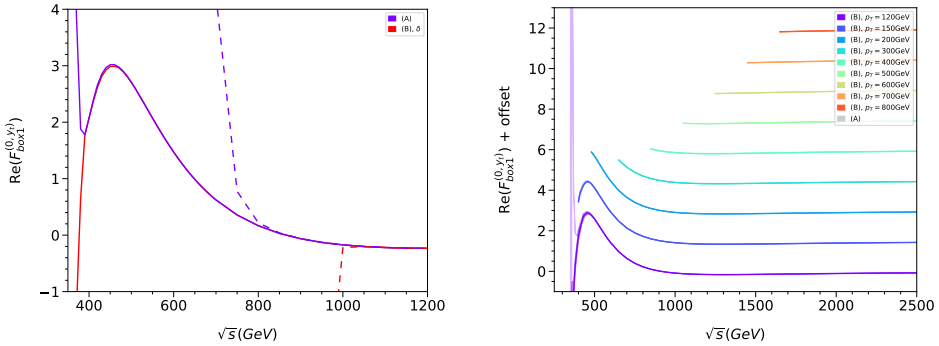

Figure 5: Real part of F_{box1} for fixed scattering angle $\theta = \pi/2$ (left) and different fixed p_T values (right). For the fixed p_T plot, an offset is applied such that the curves with different p_T are separated. (from Ref. [17])

with $e = \sqrt{4\pi\alpha}$ and external Higgs fields renormalisation, both in the on-shell scheme (G_μ scheme). Note that ξ_W and ξ_Z drop out in renormalised amplitudes. For the numerical evaluation, we use the inputs $m_t = 172$ GeV , $m_H = 125$ GeV , $m_W = 80$ GeV , $m_Z = 91$ GeV , and introduce the ratio parameter $\rho_{p_T} = \frac{p_T^H}{\sqrt{s}}$. In the following we choose $\rho_{p_T} = 0.1$ and consider the squared matrix element $\mathcal{U}_{\text{ggHH}} = \mathcal{U}^{(0)}_{\text{ggHH}} + \frac{\alpha}{\pi}\mathcal{U}^{(0,1)}_{\text{ggHH}}$ for $gg \to HH$ and $\mathcal{U}_{\text{gggH}} = \mathcal{U}^{(0)}_{\text{gggH}} + \frac{\alpha}{\pi}\mathcal{U}^{(0,1)}_{\text{gggH}}$ for $gg \to gH$. For definitions of matrix elements and their prefactors, please refer to Ref. [12]. The LO and NLO EW numerical results are shown in Fig. 3 for $gg \to HH$ and Fig. 4 for $gg \to gH$. For both processes, our large-m_t expansions yield reasonable predictions for the $\sqrt{s} \lesssim 290$ GeV region. We observe that the EW corrections for $gg \to HH$ are sizeable in the low-energy region, lifting the di-Higgs destructive interference effects which is present at the LO. The EW corrections for $gg \to gH$ are relatively small.

High-energy expansion: We perform the analytic high-energy expansion for the two-loop leading Yukawa corrections for HH production. We consider two approaches with the following hierarchies: (A) $s, t \gg m_t^2 \gg (m_H^{\text{int}})^2, (m_H^{\text{ext}})^2$ and (B) $s, t \gg m_t^2 \approx (m_H^{\text{int}})^2 \gg (m_H^{\text{ext}})^2$, where m_H^{int} and m_H^{ext} are internal and external Higgs masses respectively. We employ `exp` for amplitude-level expansions, differential equations and power-log ansatz methods for master integrals, and compute the boundary master integrals in the high-energy limit using `AsyInt` [28]. Through this procedure, we obtain analytic results for the amplitudes expanded up to order m_t^{120}. For the numerical evaluation, we employ the Padé approximation to enlarge the radius of convergence of our results. We show results for the real part of box-type form factor of F_1 for fixed transverse momentum p_T and fixed scattering angle in Fig. 5. For the fixed scattering angle plot, the solid curves represent Padé results with uncertainty bands and the dashed curves show naive expansions. We observe the central value of Padé results agree in both approaches down to $\sqrt{s} \approx 400$ GeV.

4. Conclusion

In these proceedings, we have summarised our recent contributions to NLO QCD and EW corrections for loop-induced Higgs bosons production at the LHC. These include the QCD and EW corrections for H + jet production, QCD corrections for H + 2 jets production, and EW corrections for HH production. For QCD corrections, we have conducted dedicated studies on the top-quark

mass effects for H + jet and H + 2 jets production. These effects are crucial for making precise predictions of loop-induced Higgs boson production at the NLO accuracy. For EW corrections, we have performed analytic expansions for H + jet and HH production in different kinematic regions. These results provide a good approximation across a vast range of phase space regions, showing a promising prospects for analytic higher-order EW calculations.

Acknowledgments

H.Z. would like to thank Joshua Davies, Go Mishima, Kay Schönwald, Matthias Steinhauser, Xuan Chen, Alexander Huss, Stephen Jones, Matthias Kerner, Jean-Nicolas Lang, and Jonas Lindert for collaborations on projects reported in this contribution. H.Z. is supported by the Deutsche Forschungsgemeinschaft (DFG, German Research Foundation) under grant 396021762 — TRR 257 "Particle Physics Phenomenology after the Higgs Discovery".

References

[1] LHC Higgs Cross Section Working Group collaboration, 1610.07922.
[2] A. Greljo, G. Isidori, J. M. Lindert, D. Marzocca and H. Zhang, *Eur. Phys. J. C* **77** (2017) 838 [1710.04143].
[3] H. Abouabid, A. Arhrib, D. Azevedo, J. E. Falaki, P. M. Ferreira, M. Mühlleitner and R. Santos, *JHEP* **09** (2022) 011 [2112.12515].
[4] S. Iguro, T. Kitahara, Y. Omura and H. Zhang, *Phys. Rev. D* **107** (2023) 075017 [2211.00011].
[5] S. P. Jones, M. Kerner and G. Luisoni, *Phys. Rev. Lett.* **120** (2018) 162001 [1802.00349].
[6] X. Chen, A. Huss, S. P. Jones, M. Kerner, J. N. Lang, J. M. Lindert and H. Zhang, *JHEP* **03** (2022) 096 [2110.06953].
[7] R. Bonciani, V. Del Duca, H. Frellesvig, M. Hidding, V. Hirschi, F. Moriello, G. Salvatori, G. Somogyi and F. Tramontano, *Phys. Lett. B* **843** (2023) 137995 [2206.10490].
[8] M. Niggetiedt and M. Wiesemann, 2407.01354.
[9] M. Czakon, F. Eschment, M. Niggetiedt, R. Poncelet and T. Schellenberger, 2407.12413.
[10] M. Bonetti, E. Panzer, V. A. Smirnov and L. Tancredi, *JHEP* **11** (2020) 045 [2007.09813].
[11] J. Gao, X.-M. Shen, G. Wang, L. L. Yang and B. Zhou, *Phys. Rev. D* **107** (2023) 115017 [2302.04160].
[12] J. Davies, K. Schönwald, M. Steinhauser and H. Zhang, *JHEP* **10** (2023) 033 [2308.01355].
[13] S. Di Noi, R. Gröber and M. K. Mandal, 2408.03252.
[14] U. Haisch and M. Niggetiedt, 2408.13186.
[15] B. C. Aveleira, G. Heinrich, M. Kerner and L. Kunz, 2409.05728.
[16] S. Borowka, C. Duhr, F. Maltoni, D. Pagani, A. Shivaji and X. Zhao, *JHEP* **04** (2019) 016 [1811.12366].
[17] J. Davies, G. Mishima, K. Schönwald, M. Steinhauser and H. Zhang, *JHEP* **08** (2022) 259 [2207.02587].
[18] M. Mühlleitner, J. Schlenk and M. Spira, *JHEP* **10** (2022) 185 [2207.02524].
[19] G. Heinrich, S. Jones, M. Kerner, T. Stone and A. Vestner, 2407.04653.
[20] H. T. Li, Z.-G. Si, J. Wang, X. Zhang and D. Zhao, 2407.14716.
[21] H. Zhang, K. Schönwald, M. Steinhauser and J. Davies, *PoS* **LL2024** (2024) 014 [2407.05787].
[22] H.-Y. Bi, L.-H. Huang, R.-J. Huang, Y.-Q. Ma and H.-M. Yu, *Phys. Rev. Lett.* **132** (2024) 231802 [2311.16963].
[23] A. Gehrmann-De Ridder, T. Gehrmann and E. W. N. Glover, *JHEP* **09** (2005) 056 [hep-ph/0505111].
[24] F. Buccioni, J.-N. Lang, J. M. Lindert, P. Maierhöfer, S. Pozzorini, H. Zhang and M. F. Zoller, *Eur. Phys. J. C* **79** (2019) 866 [1907.13071].
[25] S. Borowka, G. Heinrich, S. Jahn, S. P. Jones, M. Kerner, J. Schlenk and T. Zirke, *Comput. Phys. Commun.* **222** (2018) 313 [1703.09692].
[26] F. Maltoni, E. Vryonidou and M. Zaro, *JHEP* **11** (2014) 079 [1408.6542].
[27] H. Zhang, *PoS* **EPS-HEP2023** (2024) 393 [2310.14314].
[28] H. Zhang, *JHEP* **09** (2024) 069 [2407.12107].